energies

MDPI

Article

Neighborhood Effects in Wind Farm Performance: A Regression Approach

Matthias Ritter *,†, Simone Pieralli †,‡ and Martin Odening

Department of Agricultural Economics, Faculty of Life Sciences, Humboldt-Universität zu Berlin, Philippstr. 13, 10115 Berlin, Germany; Simone.PIERALLI@ec.europa.eu (S.P.); m.odening@agrar.hu-berlin.de (M.O.)

* Correspondence: matthias.ritter@agrar.hu-berlin.de; Tel.: +49-30-2093-46851

† These authors contributed equally to this work.

‡ The author works now at the European Commission, Joint Research Centre. The views expressed are purely those of the author and may not in any circumstances be regarded as stating an official position of the European Commission.

Academic Editor: Frede Blaabjerg

Received: 19 January 2017; Accepted: 9 March 2017; Published: 16 March 2017

Abstract: The optimization of turbine density in wind farms entails a trade-off between the usage of scarce, expensive land and power losses through turbine wake effects. A quantification and prediction of the wake effect, however, is challenging because of the complex aerodynamic nature of the interdependencies of turbines. In this paper, we propose a parsimonious data driven regression wake model that can be used to predict production losses of existing and potential wind farms. Motivated by simple engineering wake models, the predicting variables are wind speed, the turbine alignment angle, and distance. By utilizing data from two wind farms in Germany, we show that our models can compete with the standard Jensen model in predicting wake effect losses. A scenario analysis reveals that a distance between turbines can be reduced by up to three times the rotor size, without entailing substantial production losses. In contrast, an unfavorable configuration of turbines with respect to the main wind direction can result in production losses that are much higher than in an optimal case.

Keywords: wind energy; wake modeling; wind farm design

1. Introduction

Turbine density is a crucial parameter when designing the layout of wind farms. Optimizing turbine density must consider the trade-off between two productivity indicators: the generated energy per turbine and the generated energy per area. In most industrialized countries, land that can be used for wind energy production is scarce and costly. This scarcity calls for a high turbine density per area. On the other hand, it is well-known that, as the turbine density increases, the productivity per turbine decreases, due to the wake effects of neighboring turbines, i.e., each turbine absorbs part of the incoming wind energy, reduces the wind speed, and creates turbulences in the downstream direction. Quantification of this wake effect, however, is challenging, because of the complex aerodynamic nature of the interdependencies of turbines within a wind farm. In this article, we focus on neighborhood effects within a wind farm. Another strand of literature considers the interdependencies among wind farms on a larger regional scale (e.g., [1,2]). Many attempts have been made to estimate wind power losses by means of wake effect models. [3–5] provide an overview of the various modeling approaches. [6] distinguishes between explicit (kinematic) wake models that provide closed-form expressions for the velocity deficit and implicit models (field models) that are based on approximations of Navier-Stokes or vorticity equations. Examples of the first model type are the Jensen model [7], the Frandsen model [8], and the Larsen model [9]. The second model class is

comprised of the Eddy-viscosity by [10], the Fuga model by [11], and the large eddy simulation models by [12]. These models largely differ in their complexity and computational burden. A validation of their wake profiles and a comparison with data from field experiments can be found in [5,13].

Once a wake model has been chosen and specified, it can be used to optimize the layout of wind farms, which aims to optimally position the turbines such that the expected power production is maximized [14]. Several optimization procedures have been suggested to solve the layout problem, including mathematical programming (e.g., [15]), Monte Carlo Simulation [16,17], genetic algorithms [18], or multi-objective programming [19]. An overview of these methods and their applications is given in [20]. Most of the aforementioned approaches for optimizing the wind farm layout resort to simple wake models, particularly the Jensen model (cf. [21]). The reason for this is that the Jensen model expresses the velocity deficit δv due to the wake of a (single) turbine as a simple function of the downstream rotor radius r_d, the downwind distance d, the axial induction factor a, and a measure of the velocity of wake expansion η [22], given by:

$$\delta v = \frac{2a}{1 + \eta\left(\frac{d}{r_d}\right)^2} \tag{1}$$

The wind deficit δv can then be directly incorporated into the objective function of the optimization procedures. Equation (1) constitutes a single wake model and has to be extended to a multi-wake model that accounts for the superpositions of individual turbine wakes in a wind farm. An early attempt was made by [23], who proposed a model for the cumulative velocity deficit based on the linear superposition of individual wind deficits. Later, [24] suggested the use of squared, instead of linear, velocity deficits. According to [24], the single wakes of turbines j that affect turbine i, $W(i)$, can be aggregated through a Euclidean norm to obtain the total velocity deficit of a turbine in position i as:

$$\delta V_i = \sqrt{\sum_{j \in W(i)} \delta v_j^2} \tag{2}$$

Alternative wake adding methods are described in [25] and a comparison of the predictions from various models with actual wind farm losses can be found in [5].

The second reason for the widespread use of simple kinematic models is the fact that they are considered as fair approximations to statistically measured power losses, despite their simplicity [26]. This view, however, has been challenged. References [21,27] criticize the top hat distribution of the velocity deficit implied by the Jensen model and replace it by a Gaussian distribution to attain a better fit of the experimental data. Reference [28] reports that for two off-shore wind farms, the Jensen model underestimates production in the first few turbine rows of the wind farms, yet it overestimates production in the last few turbine rows. Reference [29] proposes a generalization of the multi-wake model (2) that considers a partial overlap of the wake area and the rotor swept area.

In this paper, we propose an alternative method to estimate power losses from wake effects for a wind farm. Instead of deriving a functional form for the velocity deficit from aerodynamic relations, we pursue an empirical, data-driven approach, which links the basic determinants of velocity losses, such as the entering wind speed, turbine alignment angle, and distance between turbines, in a flexible way and applies regression techniques to estimate the parameters of the model. The advantage of this proposed approach is that it only relies on a few assumptions and it can be adapted to any wind farm design with turbines of the same type. In this paper, we demonstrate the specification and estimation of the regression model for two wind farms in Germany.

This is not the first time that turbine interaction effects in wind farms have been estimated with statistical methods. Reference [30] was among the first to consider the neighboring effects when predicting the wind speed and power output of a wind farm. Reference [31] proposes a spatio-temporal wind forecast model that accounts for spatial wind power correlations. Recently, reference [32] estimated the power production of a wind farm using a spatial lag model with panel data. Wake effects

are implicitly captured by an interaction parameter. The contribution of our paper to the existing literature is the focus on power losses within an existing wind farm. Moreover, we aim to explain the observed power losses by means of fundamental variables. In contrast to other regression models, we explicitly take into account the relative position of individual turbines in a wind farm. Hence, our approach can be considered as a hybrid model that combines elements of engineering wake models and empirical models.

2. Methods

Following several steps, we proceeded to estimate the power loss of a wind farm due to wake effects. First, we estimated the wind velocity deficit of a single turbine, which is affected by one or more turbines in the wind farm. To this end, we approximated aerodynamic engineering models with a simple regression model, which allows for the inclusion of multiple turbine wake effects, but is parsimonious in its specification and is applicable to any wind farm design with turbines of the same type. The resulting velocity deficit was then translated to a power loss via a given power curve. We do not directly explain the power losses since they might be caused by factors other than wake effects. Finally, the power losses of all individual turbines in a wind farm were aggregated. In what follows, we describe this procedure in detail.

We modeled the velocity deficit of a turbine i at time t, δV_{it}, as a function of three variables that are suggested by engineering wake models. These three variables are: the entering (undisturbed) wind speed, u_t^∞; the distance between a disturbing turbine j and a disturbed turbine i, d_{ij}; and the turbine alignment angle between a disturbing turbine j and a disturbed turbine i, $\alpha_{ij,t}$. The turbine alignment angle describes the positioning of two turbines, depending on the wind direction: For an angle $\alpha_{ij,t_1} = 0°$, the disturbing turbine stands upwind directly in front of the disturbed turbine and thus causes a maximum wake effect at the disturbed turbine (see the upper part of Figure 1). For a different wind direction at time t_2 (the lower part of Figure 1), the angle α_{ij,t_2} describes the deviation from the previous situation of perfect alignment [33]. The higher the angle $\alpha_{ij,t}$, the lower the disturbance on turbine i caused by turbine j, maintaining a fixed distance d_{ij}. Due to the dependence on the wind direction, the turbine alignment angles $\alpha_{ij,t}$ depend on time and the position of the turbines. Note that we only considered the center of the neighboring turbine as cause for the wake effect and not the full diameter. Physically, this is not fully correct, but an incorporation of a range of turbine alignment angles spanning the full diameter would unnecessarily complicate the analysis. The undisturbed wind speed u_t^∞ is the same for all turbines and only depends on time t, whereas the distance between turbines i and j, d_{ij}, is determined by the position of the turbines. We refrained from including turbine specifications such as the rotor radius or the hub height into the model, since we only applied the model to data of the same turbine type, resulting in constant variables.

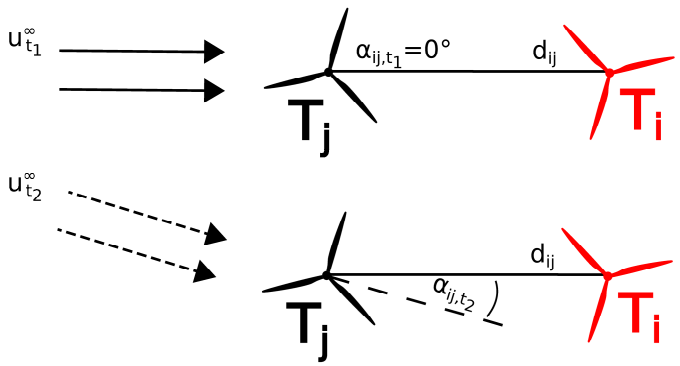

Figure 1. Explanation of the turbine alignment angle $\alpha_{ij,t}$ and distance d_{ij} for two wind directions.

To measure the effect of relevant turbines at every moment and to allow for the observations to be comparable, we did not consider fixed neighbors. Instead, we sorted neighboring turbines according

to their impact on the disturbed turbine. Otherwise, with fixed neighbors, we would only find the average effect of each turbine, which is specific to a particular wind farm design and wind conditions, and therefore, cannot be generalized. To sort relevant neighbors, we first delimited the radius of potential influence of the disturbing turbines to 1 km. This distance represents approximately 10 to 12 times the rotor diameters of typical turbines, and most kinematic models predict negligible losses for larger distances. Then, we sorted the remaining turbines by their turbine alignment angle, i.e., the neighbor within a radius of 1 km with the lowest angle was assumed to be the one causing the most disturbance. Here, we did not distinguish whether the turbine was standing on the left or right side compared to the wind direction, i.e., we consider the absolute value of the angles. In summary, the distance determined whether a turbine belongs to the group which is causing disturbance and the angle is used to sort such turbines by their influence. As an alternative to this sorting procedure, one could use a more sophisticated combination of the distance and angle to find the turbine(s) causing the most disturbance. However, for this purpose, we would have already had to assume a specific wake model, which we wanted to derive at a later stage.

Figure 2 depicts the exemplary case of one turbine disturbed by three neighbors within a 1 km radius, given a certain wind direction. Figure 2 illustrates the angles $\alpha_{01,t} - \alpha_{03,t}$ and distances $d_{01} - d_{03}$ from the disturbing turbines $T_1 - T_3$ to the disturbed turbine T_0. In this example, the wind u_t^∞ comes from the left (black arrows) and we consider the loss of turbine T_0. Turbine T_1 is assumed to be the most disturbing neighbor since the angle $\alpha_{01,t}$ is the smallest, followed by Turbine T_2 and T_3 as the second and third most disturbing turbines, respectively.

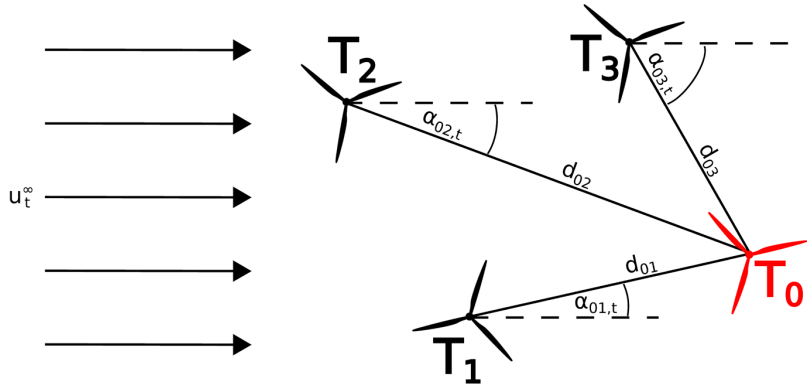

Figure 2. Definition of the distance and turbine alignment angle in the regression model.

This sorting depends on the current wind direction, i.e., it is different for a different wind direction at another time t. This implies that the distances to the (relative) neighbors also become time dependent. Moreover, we calculated the wake effect loss for each turbine separately, using the same sorting procedure. If we consider the loss of turbine T_3 in Figure 2, for example, T_2, T_1, and T_0 are the first, second, and third most disturbing neighbors for this wind direction, respectively.

We used a fully interacted linear regression model to relate the velocity deficit to the explanatory variables. In our models, we confined the analysis to one or two disturbing neighboring turbines. Ref. [22] shows that the inclusion of more than the closest disturbing turbine does not have a significant effect on the velocity deficit, i.e., the marginal effect of more than one turbine is low. Further empirical evidence for this finding is provided by [34]. Moreover, our regression model would have inflated considerably if we had included more than two neighboring turbines. While such an extension would be numerically feasible, we would likely end up with a large portion of insignificant parameter estimates and the interpretation of the results would become complicated.

Instead, our idea was to develop a parsimonious model. In the case of a single disturbing turbine (i.e., a single wake model), the specification of the model for the losses of turbine T_0 was as follows:

$$\begin{aligned} \delta V_0 &= f(\alpha_{01}, d_{01}, u^\infty) \\ &= \beta_1\alpha_{01} + \beta_2 d_{01} + \beta_3\alpha_{01}d_{01} + \beta_4\alpha_{01}u^\infty + \beta_5 \mathrm{d}_{01}u^\infty + \beta_6\alpha_{01}d_{01}u^\infty + \beta_7 u^\infty + \epsilon, \end{aligned} \tag{3}$$

where $\beta_1, \ldots, \beta_7$ are the parameters to be estimated for the most disturbing neighboring turbine and ϵ denotes the error term. To simplify the notation, we omitted the index of time t. In the case of two disturbing neighbors, a two-wake model was constructed by adding a similar expression, as in Equation (3), for the second turbine:

$$\begin{aligned} \delta V_0 &= f(\alpha_{01}, d_{01}, \alpha_{02}, d_{02}, u^\infty) \\ &= \beta_1\alpha_{01} + \beta_2 d_{01} + \beta_3\alpha_{01}d_{01} + \beta_4\alpha_{01}u^\infty + \beta_5 d_{01}u^\infty + \beta_6\alpha_{01}d_{01}u^\infty + \beta_7 u^\infty \\ &\quad + \beta_8\alpha_{02} + \beta_9 d_{02} + \beta_{10}\alpha_{02}d_{02} + \beta_{11}\alpha_{02}u^\infty + \beta_{12}d_{02}u^\infty + \beta_{13}\alpha_{02}d_{02}u^\infty + \epsilon. \end{aligned} \tag{4}$$

In the two-wake-model, the linear wind variable only enters the model once, to avoid multicollinearity. The use of a simple linear regression model may appear restrictive at first glance, in contrast with engineering wake models; however, the inclusion of interaction terms allows for the impact of the three explanatory variables to be nonlinear. Using interaction terms is also advisable because the three variables jointly unfold their impact. For example, a low distance and small angle are only relevant if there is wind. In the same manner, the wind speed passing through two different disturbing turbines has a different interaction effect on the wind deficit of the disturbed turbine. Once the model parameters have been estimated, standard statistical procedures can be applied to test the significance of the parameter estimates and the model's goodness of fit.

Even though we are interested in economic losses caused by turbine interaction in a wind farm, we first estimated the wind velocity deficits, rather than the power losses. The reason for this is that power losses may be caused by reasons other than the wakes of other turbines. Reference [35] shows that empirically observed productivity losses are often rooted in various kinds of turbine errors, such as icing or maintenance. Since it is difficult to disentangle these effects without detailed information on the error status of turbines, we decided to derive power losses by inserting observed (or estimated) wind velocities into the turbine's power curve (cf. [36]). The aggregation of power losses to the level of the wind farm was carried out by calculating the predicted losses for all N turbines occurring at every moment t in a wind farm, in the following way:

$$\delta\hat{P}_t = \sum_{i=1}^{N} \left[P(u_t^\infty) - P\left(u_t^\infty - \delta\hat{V}_{it}\right) \right] \tag{5}$$

where $\delta\hat{P}_t$ denotes the estimated power loss for the whole wind farm at time t and $\delta\hat{V}_{it}$ denotes the estimated velocity deficit for turbine i at time t. $P(\cdot)$ denotes the power curve, which converts the velocities into the expected power.

The results of the regression model can be used to predict losses for hypothetical wind farm designs. Based on historical wind speeds and absolute wind directions observed every 10 min, we calculated the distances and turbine alignment angles for each turbine, considering its position within the wind farm. For every turbine, we then decided on the number of disturbing neighbors. If there was no disturbing neighbor, we set the wind deficit and power loss to zero. For one or two disturbing turbines, plugging the distances, angles, and wind speeds into the corresponding estimated wake regression model (a single-wake or two-wake model) yielded the wind velocity deficit for the disturbed turbine at a particular moment. The undisturbed wind speeds and turbine-specific disturbed wind speeds were then plugged into the power curve to obtain the wake effect power losses. This calculation was repeated for all turbines in the wind farm at every moment and was then

calculated for the whole wind farm. These losses can be further aggregated by turbines to study the losses of different turbines within the farm.

3. Materials

We applied the estimation procedure described above to two onshore wind farms located in Bavaria (wind farm A) and Saxony-Anhalt (wind farm B), both of which are located in Germany. The exact locations and the names of the wind farms are concealed here, due to the confidentiality of the data. They are comprised of seven turbines of type Enercon E-82 (Enercon, Aurich, Germany) and of twelve turbines of type Fuhrländer FL2500 (Fuhrländer, Liebenscheid, Germany), respectively, with differing hub heights and diameters. Details on the turbine specifications are provided in Table 1, and the positioning of the turbines in the two farms is depicted in Figure 3. Wind farm A is located along the southwest-northeast direction and its turbines have an average distance of 713 m (equivalent to 8.7 rotor diameters). Wind farm B is located in a rectangle with an average distance of 657 m (equivalent to 6.6 rotor diameters). Due to these differences, it can be expected that both wind farms have different wake effects, even under similar topographic conditions. In particular, we predicted that wind farm A would be more sensitive to changes in the wind direction than wind farm B.

Table 1. Details on wind farms A and B.

Characteristics	Wind Farm A	Wind Farm B
Location	Bavaria	Saxony-Anhalt
Number of turbines	7	12
Turbine type	Enercon E-82	Fuhrländer FL2500
Turbine capacity	2.3 MW	2.5 MW
Turbine hub height	138 m	100 m
Turbine diameter	82 m	100 m

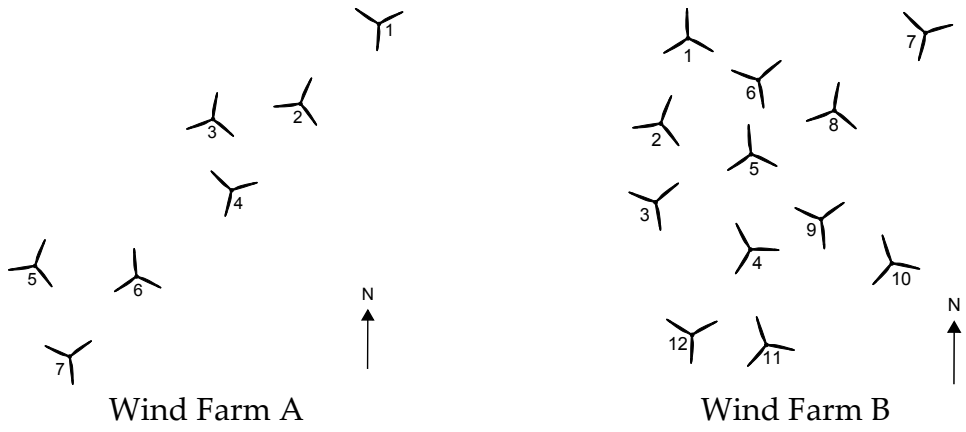

Figure 3. Turbine configuration of wind farm A and B.

Data for both wind farms are comprised of the exact coordinates for each turbine and their Supervisory Control and Data Acquisition (SCADA) data. SCADA data have the advantage of providing turbine-specific information on a low temporal scale. This is particularly useful for wake effect analyses [4]. Moreover, SCADA data are true observations, so the wake effect can be studied under realistic conditions. SCADA data contain average wind speeds over 10 min for each turbine for the time period 1 January 2014–31 March 2014 (wind farm A) and 14 November 2009–31 December 2013 (wind farm B). For wind farm A, we also obtained data on the nacelle position of each turbine, which we averaged for each moment to obtain a proxy for wind direction. Ref. [37] points out that the use of the nacelle position may cause wind direction uncertainty, due to a yaw misalignment of the turbine. For wind farm B, no direction data were available, so we had to match the observed SCADA

data with reanalysis wind direction data from Modern Era Retrospective-Analysis for Research and Applications (MERRA, cf. [38]), following [39]. The turbine alignment angles and distances were then calculated, depending on the wind speed for each moment and every turbine. For the data on the undisturbed wind speed, we took the maximum velocity measured by nacelle-mounted anemometers from all of the turbines at every moment, since there was no undisturbed meteorological mast available. This is a reasonable approximation because at least one turbine should always be undisturbed by a wake effect and is therefore supposed to have the highest mast wind speed in the wind farm.

To obtain a rather homogenous dataset and to measure the pure wake effect, we performed several data cleaning steps. First, we excluded all observations where the undisturbed mast wind speed was below 4 m/s or above 14 m/s, i.e., the rather constant parts in the power curves. For these observations, the wake effect is close to zero, since wind deficits do not lead to production differences: The observed wind speeds lie either below the cut-in speed or above the rated wind speed, where maximum production is reached. Second, only those observations were considered where the wind speed data for all of the turbines were available. Third, since we want to study the wind speed deficits caused by the wake effect, we excluded all observations where the turbine alignment angle with the first or second most disturbing neighbor was higher than $\pm 30^\circ$. This is a rather large range (we did not consider the direction of the angle, so it is 30° to the left or 30° to the right) compared to other studies. Ref. [32], for example, restricted their analysis to observations within $\pm 10^\circ$. One could use a larger dataset for the single-wake model by not excluding observations where the turbine alignment angle of the second neighbor is larger than 30°; however, this would lead to different datasets for the models and would not allow comparable results.

We ended up with a total of 11,670 (wind farm A) and 418,746 (wind farm B) turbine-specific observations. Table 2 presents the summary statistics of the data used in the regression. The average undisturbed wind speeds are 8.5 (wind farm A) and 8.8 m/s (wind farm B). As a result of our data confinement, the reported averages are not representative of the wind farms' average wind speeds. The average turbine alignment angle lies at 9.2° (wind farm A) and 8.2° (wind farm B) for the first neighbor, and at 17.7° (wind farm A) and 17.8° (wind farm B) for the second neighbor. By construction, the angle of the second turbine was always larger than that of the first turbine. Moreover, the maximum angle was 30° and maximum distance was 1 km, according to our selection procedure. Note that the first and the second neighbor show approximately the same distance on average: 0.713 km compared to 0.715 km for wind farm A, and 0.657 km compared to 0.647 km for wind farm B. This is due to the choice of the most disturbing neighbors. We see, however, that the average distance in wind farm B is lower than that in wind farm A, indicating a higher turbine density in wind farm B.

Table 2. Summary statistics of the wind farm data used in the regression.

Wind Farm	Variable	Mean	Std. Dev.	Min	Max
Wind Farm A (11,670 observations)	Velocity deficit (m/s)	1.153	0.939	0.000	9.700
	Angle 1st neighbor (°)	9.291	7.366	0.087	29.608
	Distance 1st neighbor (km)	0.713	0.219	0.326	0.963
	Angle 2nd neighbor (°)	17.694	8.190	0.392	29.813
	Distance 2nd neighbor (km)	0.715	0.207	0.326	0.963
	Undisturbed wind speed (m/s)	8.518	2.151	4.400	14.000
Wind Farm B (418,746 observations)	Velocity deficit(m/s)	1.659	1.238	0.000	9.889
	Angle 1st neighbor (°)	8.226	5.968	0.000	29.926
	Distance 1st neighbor (km)	0.657	0.187	0.320	1.000
	Angle 2nd neighbor (°)	17.809	7.089	0.300	30.000
	Distance 2nd neighbor (km)	0.647	0.209	0.320	1.000
	Undisturbed wind speed (m/s)	8.824	2.144	4.033	13.999

In both wind farms, the dominating absolute wind direction is south-west throughout most of the observed period (between 210° and 270°). As a representative display of the wind, Figure 4 depicts the wind rose distribution for wind farm B in the calendar year 2011. Because of its representativeness

of the wind conditions encountered in wind farms A and B, we will later apply this historical wind distribution to predict losses for hypothetical wind farm designs.

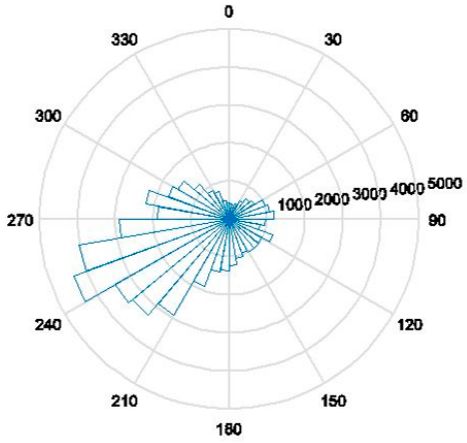

Figure 4. Histogram of wind direction in 2011.

4. Results

Regression models (3) and (4) were individually estimated for the two wind farms with Ordinary Least Squares (OLS) using STATA. For both wind farms, we specified a single-wake model and a two-wake model. These models are conservative in estimating the wind deficit between the undisturbed wind speed and the disturbed wind speed in the interior of wind farm A or B, since greater turbine alignment angles than we consider (30°) and higher numbers of neighbors might additionally cause wake effect wind deficits. The estimation results are presented in Table 3.

Table 3. Estimation results: regression coefficients.

Variable	Wind Farm A				Wind Farm B			
	Single-Wake		Two-Wake		Single-Wake		Two-Wake	
	Coeff.		Coeff.		Coeff.		Coeff.	
Angle1	0.019	***	0.001		−0.031	***	−0.036	***
Distance1	−0.823	***	−0.794	***	−0.610	***	−0.557	***
Angle1 * Distance1	0.015		0.019		0.069	***	0.063	***
Wind	0.225	***	0.245	***	0.222	***	0.246	***
Angle1 * Wind	−0.008	***	−0.006	***	−0.001		0.002	***
Distance1 * Wind	0.036	***	0.038	*	0.052	***	0.051	***
Angle1 * Distance1 * Wind	−0.0003		−0.001		−0.007	***	−0.007	***
Angle2			0.019	**			0.012	***
Distance2			−0.510	***			−0.493	***
Angle2 * Distance2			0.010				0.013	***
Angle2 * Wind			−0.005	***			−0.005	***
Distance2 * Wind			0.034				0.044	***
Angle2 * Distance2 * Wind			0.001				−0.001	
$\overline{R}$	0.723		0.727		0.702		0.704	

Note: *, **, and *** denote statistical significance at the 10, 5, and 1 percent level, respectively.

Note that the performance of the two-wake model is only slightly better than the single-wake model, i.e., the highest explanatory power comes from the most disturbing turbine. For the single-wake models, most of the coefficients are significant at the 1% level. This is also true for the two-wake model, in the case of wind farm B. In contrast, six of the 13 coefficients are not significant for wind farm A. There are also differences between the four models regarding the size and sign of the estimated parameters. While the main effect of the distance of the first neighbor is negative for all model

variants, the main effect of the angle of the first neighbor is only negative for wind farm B. Contrary to expectations, the main effect of this angle is positive for wind farm A. However, in view of the three-way interaction effects, it is difficult to assess the impact of the explanatory variables by inspection of the individual coefficients of the main effects.

To attain a better understanding of the influence of the wind speed, the turbine alignment angle, and the distance of disturbing neighboring turbines on the velocity deficit, we calculated the marginal effects of these variables while holding the other variables at their sample means (see Table 4). In line with what can be conjectured from engineering models, we found that the average marginal effect of the entering undisturbed wind speed is positive, whereas the turbine alignment angle and the distance of the most disturbing turbine have a negative effect on the wind deficit. In other words, a higher turbine alignment angle results in a lower predicted wind deficit, whereas a greater distance from the disturbing neighbor lowers the predicted wind deficit. A somewhat surprising result is the positive marginal effect of the distance of the second turbine. This might be explained by the fact that we selected the most disturbing turbines by considering their angle to the turbines which they were disturbing, but we disregarded the distance between them.

Table 4. Estimation results: average marginal effects (changes due to 1% change in variables).

Variable	Wind Farm A				Wind Farm B			
	Single-Wake		Two-Wake		Single-Wake		Two-Wake	
	Coeff.		Coeff.		Coeff.		Coeff.	
Angle1	−0.403	***	−0.346	***	−0.200	***	−0.148	***
Distance1	−0.278	***	−0.246	***	−0.084	***	−0.067	***
Angle2			−0.096	***			−0.221	***
Distance2			0.108	***			0.061	***
Wind	1.457	***	1.483	***	1.941	***	1.939	***

Note: *** denotes statistical significance at the 1 percent level, respectively.

The results of the empirical wake models are graphically displayed in Figures 5 and 6. Figure 5 depicts the velocity deficit for both wind farms when two disturbing turbines are positioned next to each other (i.e., at an angle of 90 degrees) at a distance of 500 m, whereas Figure 6 presents the simulated velocity deficits for two disturbing turbines allocated at a distance of 200 m in a line (i.e., at an angle of zero degrees). Both figures display the estimated velocity deficit at an entering wind speed of 7 m/s coming from the left. The colors indicate the extent of the velocity deficit for a turbine that is disturbed by one or two turbines. For positions where the turbine alignment angle to one disturbing turbine is lower than 30°, the results from the single-wake model are applied. For overlapping positions where angles to the first and second turbine are below 30°, the two-wake model is used with a sorting of neighbors by exact angles.

The maximal velocity deficit in Figure 5 amounts to approximately 1.5 m/s, which is a reduction of about 20 percent. The maximum wind deficit occurs directly behind the disturbing turbines. The wake effect quickly fades with an increasing distance and turbine alignment angle (i.e., a vertical movement in the graph). Comparing the two wind farms using Figure 5 reveals that the general behavior of the wake effects is similar, but that a higher level is detected in wind farm B. Moreover, the wake effect in wind farm B is more intense directly behind the turbines for larger distances (until approximately 300 m) and persists for a longer period of time with increasing distance compared to wind farm A. These differences can be explained by factors for which we do not control for in the regression approach, in particular, technical parameters such as rotor size (82 m versus 100 m) and hub height (138 m versus 100 m), as well as differences in the wind farm terrain. These differences manifest themselves in the specific regression coefficients that we estimated for each wind farm.

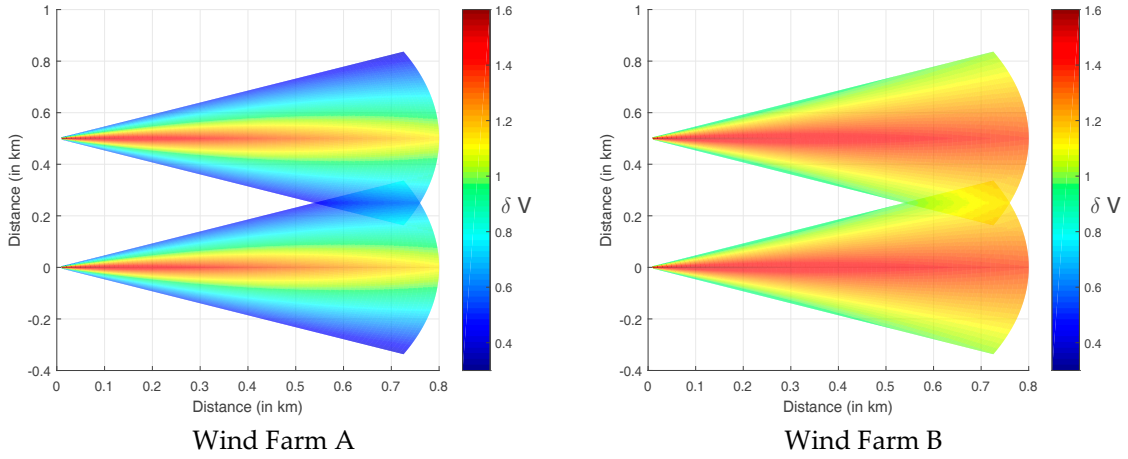

Figure 5. Simulation of velocity deficits δV with two lateral turbines for an undisturbed wind speed of 7 m/s coming from the left, wind farm A and wind farm B.

Figure 6 shows that the wake effect is aggravated by a second disturbing turbine, but that the impacts of the two disturbing turbines are not additive. As before, the wind deficit declines with an increasing distance and turbine alignment angle. Similar to Figure 5, the wake effects persist for a longer period of time in wind farm B, when increasing the downstream distance. Moreover, Figure 6 reveals a flaw in our model: The estimated wind deficit shows a discontinuity when switching from the single to the two-wake model, while in reality, the transition is expected to be smooth. This could be overcome by using a smoothening combination of the models in the transition areas.

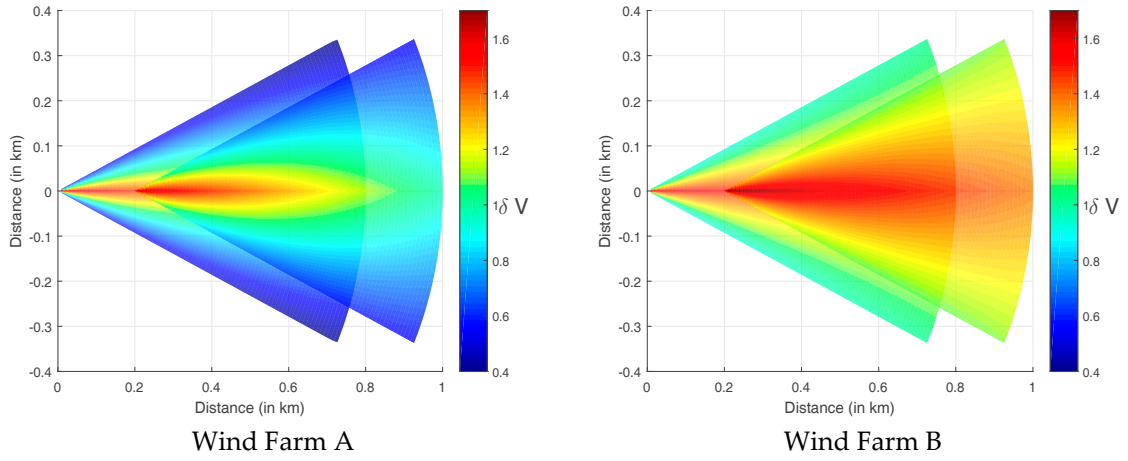

Figure 6. Simulation of velocity deficits δV with two consecutive turbines for an undisturbed wind speed of 7 m/s coming from the left, wind farm A and wind farm B.

To assess the performance of the proposed regression approach, we compared the outcome of our models with the results from a benchmark model, i.e., the model from Jensen in Equation (1). This requires the specification of the thrust coefficient, the hub height, and the surface roughness. The thrust coefficient C_T for the Enercon E-82 turbine is around 0.8 for our most frequent wind speed. Referring to the guidelines of the World Meteorological Organization [40], we chose a surface roughness length z_0 of 0.03, which corresponds to open flat terrain, grass, and few isolated obstacles.

To perform a fair comparison of the models, we conducted an out-of-sample validation. This means that we estimated the coefficients based only on a subset of the data (training data). The rest of the data were independent of the estimation and were only used for validation (testing data). As testing data, we used March 2014 (wind farm A) and the year 2013 (wind farm B), respectively.

To compare the regression model with the Jensen model, we calculated the root mean squared error (RMSE), i.e., the average deviation of the predictions of both models from the observed values:

$$\text{RMSE} = \sqrt{\frac{1}{N_{it}} \sum_{i,t} \left(\delta \hat{V}_{it} - \delta V_{it}^{\text{obs}}\right)^2} \tag{6}$$

with $\delta V_{it}^{\text{obs}}$ denoting the observed velocity deficits and N_{it} being the total number of observations.

The RMSE of our model amounts to 0.74 m/s for wind farm A and to 1.25 m/s for wind farm B. The RMSE for the Jensen model is 0.91 m/s for wind farm A and 1.42 m/s for wind farm B, which are 24% and 13% higher, respectively, than the RMSEs from our model. It becomes clear from these differences that the regression approach with a rather simple function (i.e., linear with interactions) can compete with the frequently used Jensen model, at least in this simple version with these specifications. To illustrate the sensitivity of the Jensen model to the choice of C_T and z_0, Table 5 also depicts the RMSEs for the Jensen model with different specifications: $C_T = 0.7$, $z_0 = 0.10$ (low crops, occasional large obstacles according to [40]), and $z_0 = 0.25$ (high crops, scattered obstacles). The RMSE even increases for these specifications.

Table 5. RMSE for different models.

RMSE	z_0	C_T	Velocity Deficit		Power Loss	
			Wind Farm A	Wind Farm B	Wind Farm A	Wind Farm B
Regression model	–	–	0.7391	1.2534	214.9121	446.9206
Jensen models	0.03	0.8	0.9143	1.4190	266.0114	510.3428
	0.10	0.8	0.9364	1.4711	270.3370	529.0079
	0.25	0.8	0.9611	1.5226	275.7944	546.9835
	0.03	0.7	0.9749	1.5512	278.8101	556.9284
	0.10	0.7	1.0066	1.6106	286.5066	576.9747
	0.25	0.7	1.0347	1.6625	293.5422	594.2172

The wind deficits, however, are not the best measure to describe the economic losses caused by wake effects, since the same wind loss has a different effect on the power production for different intervals of the power curve, depending on its slope. Hence, we also calculated the resulting power losses by plugging the disturbed and undisturbed wind speeds into the power curve. The RMSEs for the power losses from the regression model are 214.91 kW for wind farm A and 446.92 kW for wind farm B, whereas those for the initial Jensen model are 266.01 kW (wind farm A) and 510.34 kW (wind farm B). Thus, the RMSEs for the Jensen model are 24% and 14% higher.

To analyze the above differences in detail, Figure 7 depicts the observed and predicted power losses in the testing period against the wind speed of an (average) single turbine in wind farms A and B. For isolating the change in losses due to wind speed, we fixed the other model variables at their mean values. For every observation, i.e., for every moment and every turbine, we verified whether no, one, or two disturbing turbines were relevant, applied the appropriate regression model to calculate the predicted losses, and averaged the results for a given value of the undisturbed wind speed. Figure 7 shows that the regression model fits the observed losses rather well. For wind farm A, the regression model overestimates the observed losses in some parts, and in other parts, it underestimates them. For wind farm B, the observed losses are always underestimated by the regression model. The Jensen model, however, significantly underestimates the actual power losses for both wind farms (depicted only for $C_T = 0.8$, $z_0 = 0.03$). Figure 7 also illustrates that the regression model is able to reproduce the decrease in power losses above a wind speed of 11 m/s, due to the fact that the power curve flattens when approaching the rated wind speed.

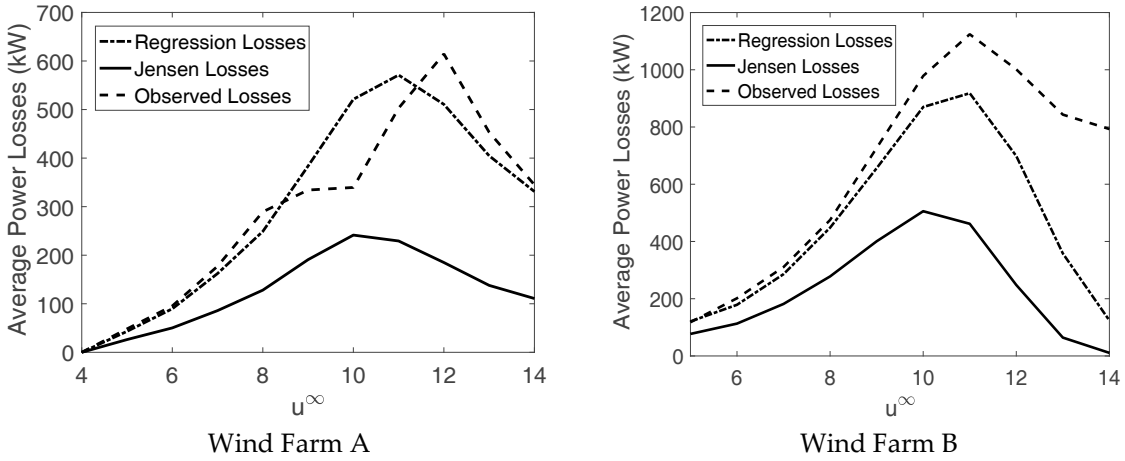

Figure 7. Wake losses as a function of wind speed, wind farm A and wind farm B.

5. Scenario Analysis

In this section, we use the regression model to simulate power losses for hypothetical wind farm designs with three turbines, given the wind speeds and wind directions every 10 min in 2011 (see Figure 4 for the histogram of the observed wind directions). Since our regression model controls for distance and the turbine alignment angle, and since we define the disturbing neighbors in a flexible manner, we are confident that our estimated regression coefficients can be used to assess the wake effects of different hypothetical layouts. This, however, is only valid if all other affecting factors, such as the turbine type, rotor diameter, or surface roughness remain constant. In the first two scenarios, we investigate the predicted change in wind deficits if the turbine density of a wind farm is increased, i.e., the distance between the turbines is reduced (see Figure 8). Scenario 1 depicts three wind turbines that are 700 m apart and located on the vertices of an equilateral triangle. A distance of 700 m approximately corresponds to the average distance in our dataset (cf. Table 2). Scenario 2 reduces the distance between the turbines from 700 m to 350 m, which still lies within the range that the regression model was calibrated for. The other two scenarios analyze the impact of the alignment of wind turbines along a specific wind direction. We consider two extreme cases: Scenario 3 presents a row of three turbines aligned in a southwest-northeast direction (245°), which is the main wind direction according to the 2011 data (see Figure 4). Scenario 4 aligns the three turbines so that they are orthogonal to the main wind direction. To evaluate the losses corresponding to these four hypothetical wind farm designs, we used the estimated regression coefficients of wind farm A from Table 3 and simulate the wind deficits for the historical wind data from 2011. We chose wind farm A because its adjusted coefficient of determination is higher than that in wind farm B, and hence, the model has a better fit to the empirical data (One might conjecture that the $\overline{R}^2$ for wind farm A is higher because the estimation is based on a shorter data set that shows less variability of wind conditions, e.g., no seasonality effects. However, the model fit is even better for wind farm A if the estimation for wind farm B is based on a comparable time period).

The results of the hypothetical scenario analyses are presented in Figure 9 for each turbine, on the left for the regression model, and on the right for the Jensen model in its initial specification. When passing from Scenario 1 to Scenario 2, i.e., when increasing the density of turbines, we see an increase in turbine-specific losses. As one would expect given our regression model and the equidistant position of the turbines in these two scenarios, the increase in losses is similar for all turbines. The Jensen model shows stronger differences between the first two scenarios, especially for the second turbine.

What appears more relevant from our analysis is the appropriate choice of the alignment direction. When changing the alignment of the turbines from being in line with the main wind direction to

orthogonal to the main wind direction (i.e., passing from Scenario 3 to Scenario 4), the losses are dramatically reduced. However, there are differences between the turbines: Turbine 1 has an excellent position regarding the main wind direction in both scenarios, so that the losses are almost equal, yet the losses for the other two turbines strongly decrease under optimal alignment. It is also worth noting that the loss of the middle turbine is always the greatest. This means that, in Scenario 3, it is worse for a turbine to be disturbed from two neighbors at two opposite sides (Turbine 2) than it is for a turbine to stand behind two turbines towards the main wind direction (Turbine 3). Similar results are obtained for the Jensen model.

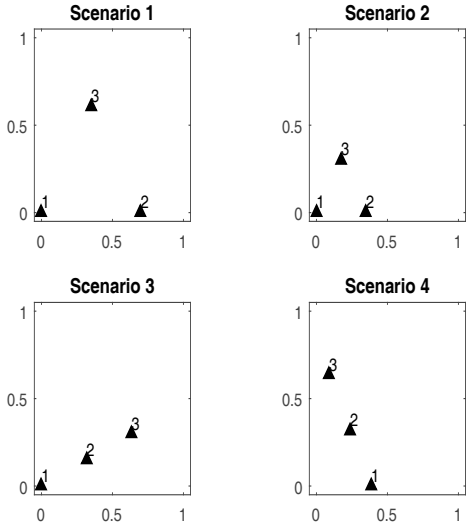

Figure 8. Layout of the hypothetical wind farm designs.

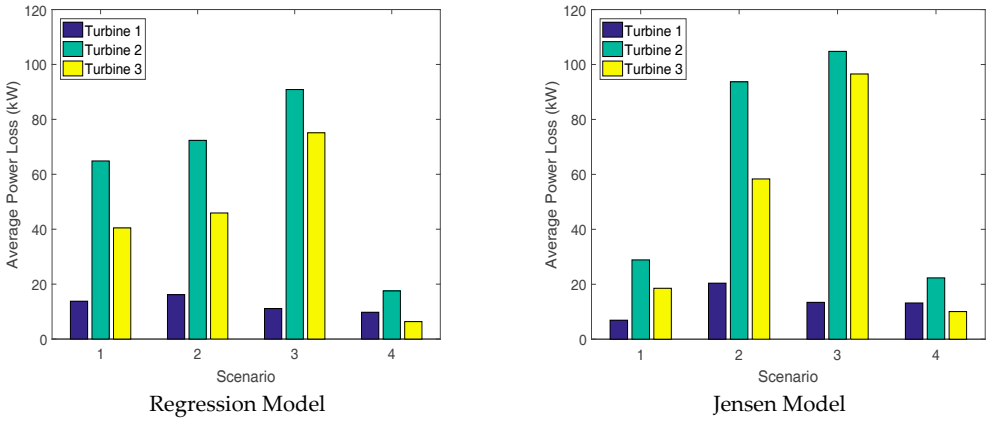

Figure 9. Results for the scenario analysis for the regression model and the Jensen model.

Table 6 depicts the losses estimated for the four wind farm designs based on the regression model. The first part shows the average 10 min losses per observation, as in the left part of Figure 9. The average losses per observation over all of the turbines are 40 kW (Scenario 1), 45 kW (Scenario 2), 59 kW (Scenario 3), and 11 kW (Scenario 4). This stresses again that in our scenarios, the alignment, with respect to the wind direction distribution, is more important than the density of the turbines.

The second part of Table 6 shows the total annual loss for the same scenarios, which means that the values per 10 min observation in kW are aggregated for the entire year and converted into MWh. These values are then compared to the maximum attainable yearly production of 5219 MWh per turbine or 15,658 MWh for all three, i.e., the hypothetical case that all three turbines are not disturbed by wake effects. An increasing turbine density from Scenario 1 to Scenario 2 leads to changes

in losses of less than 70 MWh per turbine, i.e., slightly more than one percentage point. The worst alignment (Scenario 3) leads to a loss of almost 10% for the whole wind farm. This can be reduced by factor 5 to 1.9%, with optimal alignment (Scenario 4).

Table 6. Estimated losses for hypothetical wind farms in different scenarios.

Average 10 Min Loss (in kW)	**Turbine**			**Wind Farm**
Scenario	**1**	**2**	**3**	
1	13.8	64.9	40.5	39.7
2	16.1	72.4	45.9	44.8
3	11.1	90.9	75.1	59.0
4	9.8	17.5	6.4	11.2
Total Annual Loss (in MWh)	**Turbine**			**Wind Farm**
Scenario	**1**	**2**	**3**	
1	120.7 (2.3%)	568.2 (10.9%)	354.6 (6.8%)	1043.5 (6.7%)
2	141.4 (2.7%)	633.8 (12.1%)	402.2 (7.7%)	1177.5 (7.5%)
3	97.4 (1.9%)	796.0 (15.3%)	658.0 (12.6%)	1551.4 (9.9%)
4	85.5 (1.6%)	153.6 (2.9%)	55.7 (1.1%)	294.8 (1.9%)
Attainable total production (100%)	5219.3	5219.3	5219.3	15,657.9

In summary, our analysis shows that the most important decision for wind farm design is turbine alignment. The choice of turbine alignment seems to be a more crucial decision than their density, at least for reasonable intra-turbine distances (approximately 2.5 to 3 times the turbine rotor diameter).

6. Discussion and Conclusions

In this paper, we propose a parsimonious regression approach to wake modeling that can be used to predict production losses of existing and potential wind farms. Motivated by simple engineering wake models, we use wind speed, turbine alignment angle, and distance as explanatory variables. Unlike existing wake models, our approach is mainly data driven and utilizes real world data instead of experimental data. The model is estimated for two wind farms in Germany. We find that the regression model is a good fit with observed wind deficits for both wind farms. The gain in estimation accuracy when switching from a single wake model to a two-wake model is moderate. Compared to the standard Jensen model, a reduction of the root mean square error can be attained in the empirical wake model. A scenario analysis revealed that the distance between turbines can be reduced by up to three times the rotor size, without entailing substantial production losses. In contrast, an unfavorable configuration of turbines with respect to the main wind direction can lead to five times higher production losses than in an optimal case.

Our empirical wake model is characterized by several useful features. First, the approach is rather flexible and can be easily estimated for any wind farm design. Second, due to its data driven nature, the model is able to capture the specific effects that occur in existing wind farms. In contrast to the Jensen model, which only shows two adjustable parameters (thrust coefficient and surface roughness), the regression model has many more parameters that can be tailored to specific wind farms. This advantage, however, comes at the cost of a reduced generalizability of the results: an estimated set of regression parameters can only be used for a specific turbine type. The model is also useful for predicting the effects of extending existing wind farms or changing wind conditions. Other limitations of our model stem from the fact that it produces meaningful results for only a limited range of turbine alignment angles and that discontinuities occur when mixing single and two-wake models.

There are several starting points for extending and refining the proposed empirical wake model. First of all, it would be relevant to test the model's performance for other wind farms under a variety of external conditions using other data sources, particularly meteorological mast data. From a methodological viewpoint, alternative definitions of relevant turbines, the inclusion of nonlinear terms in the explanatory variables, or the application of a Tobit regression that incorporates non-disturbing turbines into the model, could further improve the results of the model.

Acknowledgments: Financial support from the German Research Foundation through the CRC 649 "Economic Risk" is gratefully acknowledged. Moreover, the authors cordially thank 4initia GmbH for providing the data.

Author Contributions: Matthias Ritter, Simone Pieralli, and Martin Odening conceived and designed the model setup; Matthias Ritter and Simone Pieralli performed the estimation and analyzed the data; Matthias Ritter, Simone Pieralli, and Martin Odening wrote the paper.

Conflicts of Interest: The authors declare no conflict of interest. The founding sponsors had no role in the design of the study; in the collection, analyses, or interpretation of data; in the writing of the manuscript, and in the decision to publish the results.

References

1. Miller, L.M.; Brunsell, N.A.; Mechem, D.B.; Gans, F.; Monaghan, A.J.; Vautard, R.; Keith, D.W.; Kleidon, A. Two methods for estimating limits to large-scale wind power generation. *Proc. Natl. Acad. Sci. USA* **2015**, *112*, 11169–11174. [CrossRef] [PubMed]
2. Adams, A.S.; Keith, D.W. Are global wind power resource estimates overstated? *Environ. Res. Lett.* **2013**, 8. [CrossRef]
3. Crespo, A.; Hernández, J.; Frandsen, S. Survey of modelling methods for wind turbine wakes and wind farms. *Wind Energy* **1999**, *2*, 1–24. [CrossRef]
4. Barthelmie, R.J.; Pryor, S.C. An overview of data for wake model evaluation in the Virtual Wakes Laboratory. *Appl. Energy* **2013**, *104*, 834–844. [CrossRef]
5. Stevens, R.J.; Meneveau, C. Flow structure and turbulence in wind farms. *Annu. Rev. Fluid Mech.* **2017**, *49*, 311–339. [CrossRef]
6. Kiranoudis, C.T.; Maroulis, Z.B. Effective short-cut modelling of wind park efficiency. *Renew. Energy* **1997**, *11*, 439–457. [CrossRef]
7. Jensen, N. *A Note on Wind Turbine Interaction*; Technical Report No. M-2411; Risoe National Laboratory: Roskilde, Denmark, 1983.
8. Frandsen, S. On the Wind-Speed Reduction in the Center of Large Clusters of Wind Turbines. *J. Wind Eng. Ind. Aerodyn.* **1992**, *39*, 251–265. [CrossRef]
9. Larsen, G.C. *A Simple Wake Calculation Procedure*; DTU Orbit: Kongens Lyngby, Denmark, 1988.
10. Ainslie, J.F. Calculating the Flowfield in the Wake of Wind Turbines. *J. Wind Eng. Ind. Aerodyn.* **1988**, *27*, 213–224. [CrossRef]
11. Ott, S.; Berg, J.; Nielsen, M. *Wind Energy Div. Risoe-R-1772 (EN)*; Linearised CFD Models for Wakes Technical University of Denmark, Risoe National Laboratory for Sustainable Energy; Technical University of Denmark: Kongens Lyngby, Denmark, 2011; pp. 3892–3899.
12. Witha, B.; Steinfeld, G.; Dorenkamper, M.; Heinemann, D. Large-eddy simulation of multiple wakes in offshore wind farms. *J. Phys. Conf. Ser.* **2014**, *555*, 012108. [CrossRef]
13. Duckworth, A.; Barthelmie, R. Investigation and validation of wind turbine wake models. *Wind Eng.* **2008**, *32*, 459–475. [CrossRef]
14. Chowdhury, S.; Zhang, J.; Messac, A.; Castillo, L. Optimizing the arrangement and the selection of turbines for wind farms subject to varying wind conditions. *Renew. Energy* **2013**, *52*, 273–282. [CrossRef]
15. Turner, S.D.O.; Romero, D.A.; Zhang, P.Y.; Amon, C.H.; Chan, T.C.Y. A new mathematical programming approach to optimize wind farm layouts. *Renew. Energy* **2014**, *63*, 674–680. [CrossRef]
16. Brusca, S.; Lanzafame, R.; Messina, M. Wind turbine placement optimization by means of the Monte Carlo simulation method. *Model. Simul. Eng.* **2014**, *2014*, 760934. [CrossRef]
17. Marmidis, G.; Lazarou, S.; Pyrgloti, E. Optimal placement of wind turbines in a wind park using Monte Carlo simulation. *Renew. Energy* **2008**, *33*, 1455–1460. [CrossRef]

18. Emami, A.; Noghreh, P. New approach on optimization in placement of wind turbines within wind farm by genetic algorithms. *Renew. Energy* **2010**, *35*, 1559–1564. [CrossRef]
19. Kusiak, A.; Song, Z. Design of wind farm layout for maximum wind energy capture. *Renew. Energy* **2010**, *35*, 685–694. [CrossRef]
20. Asta, S. *A Survey on Recent Off-Shore Wind Farm Layout Optimization Methods*; Technical Report; University of Nottingham: Nottingham, UK, 2013.
21. Bastankhah, M.; Porte-Agel, F. A new analytical model for wind-turbine wakes. *Renew. Energy* **2014**, *70*, 116–123. [CrossRef]
22. Samorani, M. The Wind Farm Layout Optimization Problem. In *Handbook of Wind Power Systems*; Springer: Berlin/Heidelberg, Germany, 2013; pp. 21–38.
23. Lissaman, P.B.S. Energy effectiveness of arbitrary arrays of wind turbines. *J. Energy* **1979**, *3*, 323–328. [CrossRef]
24. Katic, I.; Højstrup, J.; Jensen, N.O. A Simple Model for Cluster Efficiency. In Proceedings of the European Wind Energy Association Conference and Exhibition, Rome, Italy, 7–9 October 1986; pp. 407–410.
25. Gocmen, T.; Van der Laan, P.; Rethore, P.E.; Diaz, A.P.; Larsen, G.C.; Ott, S. Wind turbine wake models developed at the technical university of Denmark: A review. *Renew. Sustain. Energy Rev.* **2016**, *60*, 752–769. [CrossRef]
26. Peña, A.; Réthoré, P.-E.; van der Laan, M.P. On the application of the Jensen wake model using a turbulence-dependent wake decay coefficient: The Sexbierum case. *Wind Energy* **2016**, *19*, 763–776. [CrossRef]
27. Niayifar, A.; Porté-Agel, F. Analytical Modeling of Wind Farms: A New Approach for Power Prediction. *Energies* **2016**, *9*, 741. [CrossRef]
28. Gaumond, M.; Réthoré, P.-E.; Bechmann, A.; Ott, S.; Larsen, G.C.; Pena Diaz, A.; Kurt, K. Benchmarking of wind turbine wake models in large offshore windfarms. In Proceedings of the Science of Making Torque from Wind, Oldenburg, Germany, 9–11 October 2012.
29. Wan, C.Q.; Wang, J.; Yang, G.; Gu, H.J.; Zhang, X. Wind farm micro-siting by Gaussian particle swarm optimization with local search strategy. *Renew. Energy* **2012**, *48*, 276–286. [CrossRef]
30. Alexiadis, M.C.; Dokopoulos, P.S.; Sahsamanoglou, H.S. Wind speed and power forecasting based on spatial correlation models. *IEEE Trans. Energy Convers.* **1999**, *14*, 836–842. [CrossRef]
31. Xie, L.; Gu, Y.; Zhu, X.; Genton, M.G. Power system economic dispatch with spatio-temporal wind forecasts. In Proceedings of the IEEE 2011 EnergyTech, Cleveland, OH, USA, 25–26 May 2011; pp. 1–6.
32. Croonenbroeck, C.; Ambach, D. Censored spatial wind power prediction with random effects. *Renew. Sustain. Energy Rev.* **2015**, *51*, 613–622. [CrossRef]
33. McKay, P.; Carriveau, R.; Ting, D.S.; Newson, T. Turbine Wake Dynamics. *Adv. Wind Power* **2012**, 65. [CrossRef]
34. Porté-Agel, F.; Wu, Y.-T.; Chen, C.-H. A numerical study of the effects of wind direction on turbine wakes and power losses in a large wind farm. *Energies* **2013**, *6*, 5297–5313. [CrossRef]
35. Pieralli, S.; Ritter, M.; Odening, M. Efficiency of wind power production and its determinants. *Energy* **2015**, *90*, 429–438. [CrossRef]
36. Barthelmie, R.J.; Hansen, K.; Frandsen, S.T.; Rathmann, O.; Schepers, J.; Schlez, W.; Phillips, J.; Rados, K.; Zervos, A.; Politis, E. Modelling and measuring flow and wind turbine wakes in large wind farms offshore. *Wind Energy* **2009**, *12*, 431–444. [CrossRef]
37. Gaumond, M.; Rethore, P.E.; Ott, S.; Pena, A.; Bechmann, A.; Hansen, K.S. Evaluation of the wind direction uncertainty and its impact on wake modeling at the Horns Rev offshore wind farm. *Wind Energy* **2014**, *17*, 1169–1178. [CrossRef]
38. Rienecker, M.M.; Suarez, M.J.; Gelaro, R.; Todling, R.; Bacmeister, J.; Liu, E.; Bosilovich, M.G.; Schubert, S.D.; Takacs, L.; Kim, G.K.; et al. MERRA: NASA's Modern-Era Retrospective Analysis for Research and Applications. *J. Clim.* **2011**, *24*, 3624–3648. [CrossRef]
39. Ritter, M.; Shen, Z.; López Cabrera, B.; Odening, M.; Deckert, L. Designing an index for assessing wind energy potential. *Renew. Energy* **2015**, *83*, 416–424. [CrossRef]
40. World Meteorological Organization. Part I, Chapter 5: Measurement of Surface Wind. In *Guide to Meteorological Instruments and Methods of Observation*; World Meteorological Organization: Geneva, Switzerland, 2010.